

LIST OF CONTENT

Chapter	Page
I INTRODUCTION.....	1
Rational for the study	1
Objectives of the study	4
Expected outputs of the study	4
II RELATED THEORITICAL	5
Piezoelectricity.....	5
Ferroelectricity	5
Typical interested properties of ferroelectric materials	8
Dielectric properties	8
Polarization	10
Hysteresis loop	11
Phase transition and Curie temperature.....	12
Typical ferroelectric materials: Barium titanate (BT).....	13
Typical preparation technique for ferroelectric ceramics.....	14
Solid state reaction method.....	14
Sol-gel method.....	15
Co-precipitation method.....	15
Hydrothermal synthesize method.....	16
Combustion technique.....	16
Sintering process.....	16
Typical characterizations for ferroelectric ceramics.....	17
Thermal analysis (DSC and TGA).....	17
X-ray diffraction (XRD).....	19
Scanning electron microscope (SEM).....	20
Transmission electron microscope (TEM).....	21

LIST OF CONTENT (CONT.)

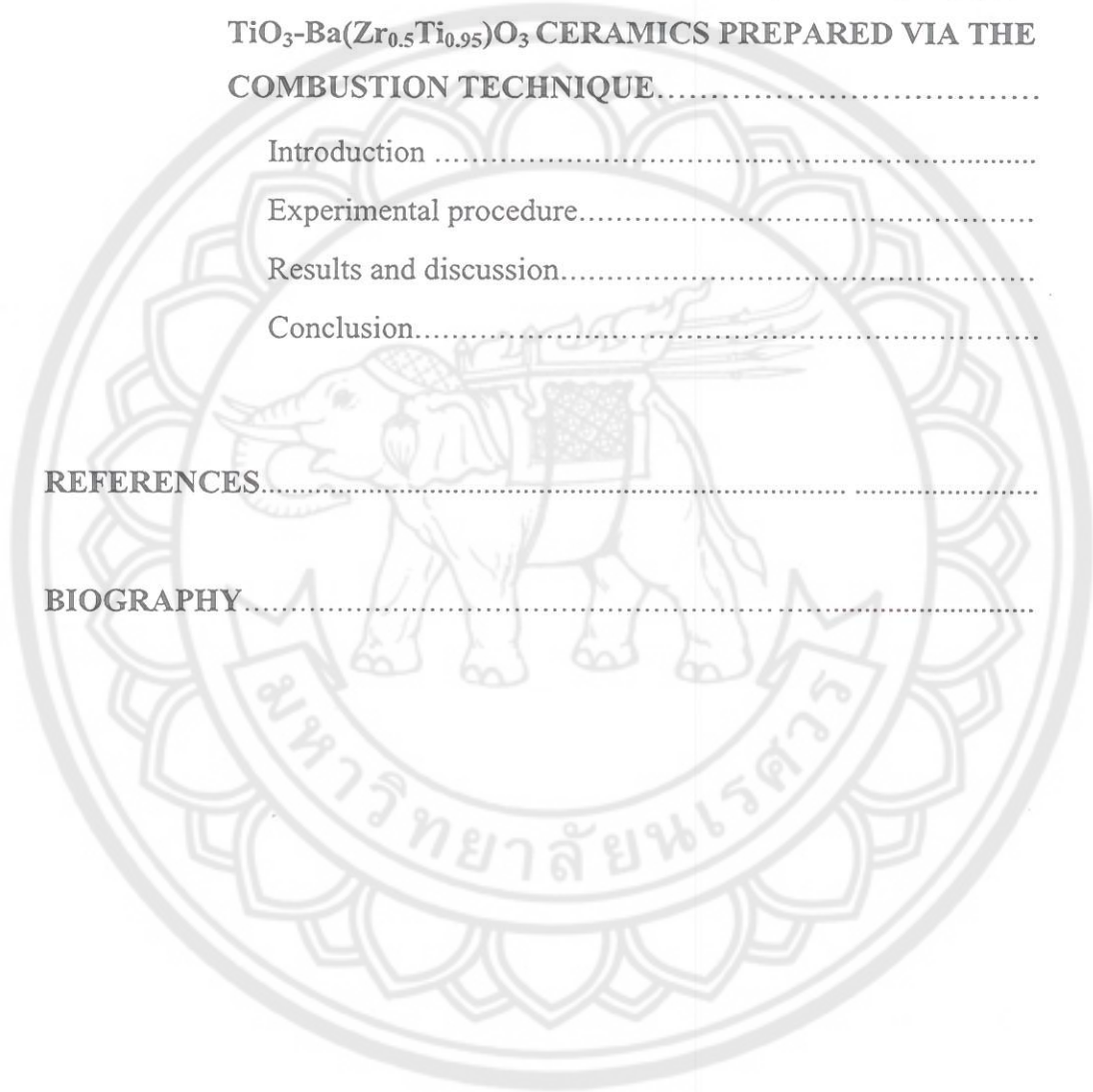
Chapter	Page
Dielectric measurement.....	22
Ferroelectric measurement.....	23
III LITERATURE REVIEW	24
Barium zirconate titanate	24
Effects of zirconium content on structure and typical properties of BZT ceramics	25
Crystal structure	25
Dielectric constant	27
Phase transition temperatures.....	29
Ferroelectric polarization.....	33
Bismuth sodium titanate ($\text{Bi}_{0.5}\text{Na}_{0.5}\text{TiO}_3$, BNT).....	35
Several techniques for improvement of BNT properties.....	36
Cation substituted BNT perovskite lattices.....	36
Binary system of BNT-based.....	40
Investigation of the combustion technique for synthesizing ferroelectric materials.....	44
Typical organic compound selection as fuel.....	44
Decomposition reaction of the typical fuel (urea).....	45
Fuel content selection.....	47
IV THE EFFECTS OF FIRING TEMPERATURES AND DWELL TIME ON PHASE FORMATION, MICROSTRUCTURE AND DIELECTRIC PROPERTIES OF $\text{BaZr}_{0.10}\text{Ti}_{0.90}\text{O}_3$ CERAMICS PREPARED VIA THE COMBUSTION TECHNIQUE.....	51

LIST OF CONTENT (CONT.)

Chapter	Page
Introduction	51
Experimental procedure.....	52
Results and discussion.....	53
Conclusion.....	68
V PHASE FORMATION, MICROSTRUCTURE AND ELECTRICAL PROPERTIES OF $\text{Ba}(\text{Zr}_x\text{Ti}_{1-x})\text{O}_3$ CERAMICS SYNTHESIZED THROUGH A NOVEL COMBUSTION TECHNIQUE.....	70
Introduction	70
Experimental procedure.....	71
Results and discussion.....	72
Conclusion.....	84
VI THE EFFECTS OF FIRING TEMPERATURES ON PHASE FORMATION, MICROSTRUCTURE AND DIELECTRIC PROPERTIES OF $\text{Bi}_{0.5}(\text{Na}_{0.74}\text{K}_{0.16}\text{Li}_{0.10})_{0.5}\text{TiO}_3$ CERAMICS SYNTHESIZED VIA THE COMBUSTIONROUTE.....	85
Introduction	85
Experimental procedure.....	86
Results and discussion.....	87
Conclusion.....	101

LIST OF CONTENT (CONT.)

Chapter	Page
VII PHASE FORMATION, MICROSTRUCTURE AND DIELECTRIC PROPERTIES OF $\text{Bi}_{0.5}(\text{Na}_{0.74}\text{K}_{0.16}\text{Li}_{0.10})_{0.5}$ $\text{TiO}_3\text{-Ba}(\text{Zr}_{0.5}\text{Ti}_{0.95})\text{O}_3$ CERAMICS PREPARED VIA THE COMBUSTION TECHNIQUE.....	103
Introduction	103
Experimental procedure.....	104
Results and discussion.....	105
Conclusion.....	112
REFERENCES.....	113
BIOGRAPHY.....	124



LIST OF TABLES

Table	Page
1 The phase transition temperature (T_1 , T_2 and T_c) of BZT ceramics	30
2 T_{r-o} , T_{o-t} and T_c as a function of zirconium content reported by literatures	32
3 The saturated polarization (P_s), remanent polarization (P_r), and coercive field (E_c) of BZT ceramics at 30 °C.....	35
4 Room-temperature dielectric and piezoelectric properties of BNT-based ceramic.....	40
5 Electrical properties of $(1-x)\text{Na}_{0.5}\text{Bi}_{0.5}\text{TiO}_3-x\text{BaTiO}_3$ or NBBT x ceramics.....	42
6 Piezoelectric, dielectric properties and density of BNT–BZT100 x ceramics	43
7 Some properties of organic compounds.....	44
8 Effects of various organic compounds and particular properties of Ni–Zn ferrite synthesized by the proposed combustion synthesis method	45
9 Comparison of powder properties with different oxidant-to-fuel ratio.....	50
10 Percent of perovskite phase and the average particle size of BZT10 Powders.....	58
11 The average grain size, density, theoretical density, dielectric properties, Curie temperature and diffuseness constant of BZT10 ceramics.....	65
12 Average grain size and density of $\text{Ba}(\text{Zr}_x\text{Ti}_{1-x})\text{O}_3$ sintered ceramics.....	77
13 The T_{o-t} , T_c , maximum dielectric constant (ϵ_r) and dielectric loss ($\tan\delta$) at T_c , and diffuseness (γ) of $\text{Ba}(\text{Zr}_x\text{Ti}_{1-x})\text{O}_3$ ceramics.....	82
14 The P_r and E_c of $\text{Ba}(\text{Zr}_x\text{Ti}_{1-x})\text{O}_3$ ceramics.....	83
15 Percent perovskite phase, lattice parameter a and average particle size of BNKLT1610 powders.....	91
16 Percent perovskite phase, lattice parameter a , average grain size and density of BNKLT1610 ceramics.....	97
17 The T_d , T_m , ϵ_d , ϵ_m , $\Delta\epsilon_{md}$, ϵ_r and $\tan\delta$ of BNKLT1610ceramics.....	101

LIST OF TABLES (CONT.)

Table		Page
18	The lattice parameters a and c , unit cell volume, c/a ratio and average grain size of BNKLT-100xBZT ceramics.....	108
19	Density, T_d , T_m , ϵ_r , ϵ_{max} and $\tan\delta$ of BNKLT-100xBZT ceramics.....	111



LIST OF FIGURES

Figures		Page
1	(a) Schematic illustration of electric dipoles with in piezoelectric materials, (b) Compressive stresses on materials cause a voltage difference (direct effect), (c) Applied voltage causes materials deform the crystal lattice (converse effect).....	6
2	Interrelationship of piezoelectric and subgroup on the basis of symmetry	7
3	Ion positions in BaTiO ₃	8
4	(a) Parallel-plate capacitor of area A and separation d in vacuum attached to a voltage source, (b) Closing of the circuit causes a transient surge of current to flow through the circuit, (c) Parallel-plate capacitor of area A and separation dielectric materials is placed between the plates, (d) Closing of the circuit results in a charge stored on the parallel plates of (c) circuit	9
5	Functional dependence of Q on applied voltage. Slope of curve is related to the dielectric constant of the material.....	9
6	A typical ferroelectric hysteresis loops	12
7	Variation of relative permittivity with temperature for BaTiO ₃ ...	12
8	The crystal structures of BaTiO ₃ (a) Above Curie point show cubic structure, (b) Below Curie point the structure is tetragonal form with Ba ²⁺ and Ti ⁴⁺ slightly shifted relative to O ²⁻	14
9	Schematic of two particles partly joined together on sintering process Characterization techniques for ferroelectric ceramics.	17
10	A typical DSC curve.....	18
11	Block diagram of a DSC instrument.....	18

LIST OF FIGURES (CONT.)

Figures		Page
12	Schematic illustration of the diffractometer method of crystal Analysis.....	20
13	Schematic diagram of the basic design of a SEM.....	21
14	The schematic outline of a TEM.....	22
15	Diagram for dielectric measurement (parallel plate method).....	22
16	Schematic of a circuit for P - E measurement.....	22
17	Schematic diagram of the Zr doped affects the phase transition temperatures of barium titanate.....	25
18	Dependences of the a - and c -axis lattice constants and c/a ratio (right hand side ordinate) on Zr/Ti ratio at room temperature	26
19	Phase identification of BZT ceramics with variation of mol% zirconium of x reported by several literatures	27
20	Temperature dependence of the relative permittivity of $Ba(Zr_xTi_{1-x})O_3$ ceramics at 1 kHz	28
21	Temperature dependence of dielectric constant ϵ at 1 kHz for the $Ba(Zr_xTi_{1-x})O_3$ ceramics with $x = 0, 0.03, 0.05, 0.08, 0.15, 0.2, 0.25$ and 0	28
22	Variation of maximum dielectric constant of $Ba(Zr_xTi_{1-x})O_3$ from literatures.....	29
23	Temperature dependence of the relative permittivity for $Ba(Zr_xTi_{1-x})O_3$ ceramics with (a) $x = 0$ sintered at 1300°C , (b) $x = 0.02$ sintered at 1350°C , (c) $x = 0.05$ sintered at 1450°C and (d) $x = 0.08$ sintered at 1400°C at 1 kHz, 10 kHz and 100 kHz.....	30
24	Phase transition temperature T_c , T_{0-t} and maximum dielectric permittivity ϵ_m as functions of zirconium content x at 10 kHz for $Ba(Zr_xTi_{1-x})O_3$ ceramics.....	31

LIST OF FIGURES (CONT.)

Figures		Page
25	<i>P-E</i> Hysteresis loops of Ba(Zr _x Ti _{1-x})O ₃ ceramics at room temperature and 1 kHz with (a) $x = 0.05$, (b) $x = 0.10$, (c) $x = 0.15$, and (d) $x = 0.20$	33
26	The E_c and P_r dependences of Zr/Ti ratio in Ba(Zr _x Ti _{1-x})O ₃ ceramics.....	34
27	<i>P-E</i> hysteresis loop at the temperatures ranging from 30 °C to 120 °C of BaZr _x Ti _{1-x} O ₃ with $x = 0.08$ sintered at 1400 °C.....	34
28	XRD patterns of BNT- x BKT powders.....	36
29	The piezoelectric constant d_{33} , electromechanical coupling factor K_p , dielectric constant at room temperature ϵ_r and $\tan\delta$ as a function of BKT content.....	37
30	The temperature dependence of ϵ_r and $\tan\delta$ of BNT- x BKT ceramics with different compositions.....	38
31	XRD patterns of Li and K substituted BNT ceramics; (a) BNT, (b) BNLT10, (c) BNKT10, (d) BNKT16, (e) BNKLT16-10 and (f) BNKLT16-35, in the 2θ range of 20–70° and 38–50°	38
32	Temperature dependences of permittivity for Li and K substituted BNT ceramics at frequency of 10 kHz.....	39
33	X-ray diffraction patterns of (1- x)Na _{0.5} Bi _{0.5} TiO ₃ - x BaTiO ₃ ceramics.....	41
34	XRD patterns of BNT-BZT100 x ceramics.....	42
35	<i>P-E</i> loops of BNT-BZT100 x ceramics with a maximum field of 40 kV/cm at room temperature.....	44
36	Typical TGA plots of the precursors prepared by using various fuel.....	45
37	TGA, DTA graphs and quantitative results of the GC/MS evolved gas analysis.....	46
38	Schematic diagram of major decomposition reaction of urea.....	47

LIST OF FIGURES (CONT.)

Figures		Page
39	TGA-DSC curves for the mixture of BZT powders and urea.....	54
40	XRD patterns of BZT10 powders calcined at various temperatures for 2 h:(ω) BaCO ₃ ; (ρ) ZrO ₂ ; (β) Ba ₂ TiO ₄	56
41	XRD patterns of BZT10 powders calcined at 1000 °C for various dwell times: (ω) BaCO ₃	57
42	XRD patterns of BZT10 at a very low scanning rate: (a) powder calcined at 800 °C for 2 h, (b) powder calcined at 1000 °C for 2 h, (c) powder calcined at 1000 °C for 5 h, (d) ceramics sintered at 1350 °C for 2 h, (e) ceramics sintered at 1400 °C for 2 h, (f) ceramics sintered at 1450 °C for 2 h.....	59
43	XRD patterns of BZT10 ceramics sintered at various temperatures.....	60
44	SEM photographs of BZT10 calcined powders for 2 h; (a) calcined at 600 °C, (b) calcined at 700 °C, (c) calcined at 800 °C, (d) calcined at 900 °C, (e) calcined at 1000 °C, (f) calcined at 1100 °C, (g) calcined at 1200 °C and (h) calcined at 1300 °C.....	62
45	TEM micrographs of BZT10 powders calcined at 1000 °C for 2 h; (a) original magnification x9700, (b) original magnification x46,000, and (c) original magnification x135,000.....	63
46	SEM photographs of BZT10 ceramics sintered at; (a) 1300 °C, (b) 1350 °C, (c) 1400 °C, and (d) 1500 °C.....	64
47	Temperature dependences of dielectric constant of BZT10 ceramics sintered at different temperature.....	67

LIST OF FIGURES (CONT.)

Figures	Page
48 The dependence of $\ln\left(\frac{1}{\varepsilon} - \frac{1}{\varepsilon_m}\right)$ versus $\ln(T - T_m)$ of BZT100x ceramics sintered with various temperatures for 2 h; (a) sintered at 1300 °C, (b) sintered at 1350 °C and (c) sintered at 1400 °C...	68
49 XRD patterns of Ba(Zr _x Ti _{1-x})O ₃ powders with 0.025 ≤ x ≤ 0.150.....	72
50 SEM photographs of Ba(Zr _x Ti _{1-x})O ₃ calcined powders; (a) x = 0.025, (b) x = 0.050, (c) x = 0.075, (d) x = 0.100, (e) x = 0.125 and (f) x = 0.150.....	73
51 TEM images of Ba(Zr _x Ti _{1-x})O ₃ calcined powders; (a) x = 0.050, (b) x = 0.100 and (c) x = 0.150.....	74
52 XRD patterns of Ba(Zr _x Ti _{1-x})O ₃ ceramics with 0.025 ≤ x ≤ 0.150; (a) at 2θ of 10-60° and (b) slow scanning rate at 2θ of 72-77°.....	75
53 The SEM micrographs of Ba(Zr _x Ti _{1-x})O ₃ sintered ceramics; (a) x = 0.025, (b) x = 0.050, (c) x = 0.075, (d) x = 0.100, (e) x = 0.125 and (f) x = 0.150.....	76
54 Temperature dependences of dielectric constant of BZT100x ceramics where 0.025 ≤ x ≤ 0.150.....	78
55 Dielectric loss curve of the BZT100x ceramics where 0.025 ≤ x ≤ 0.150.....	78
56 Phase transition temperature T _{o-1} and T _c as function of zirconium content x for Ba(Zr _x Ti _{1-x})O ₃ ceramics.....	78
57 The dependence of $\ln\left(\frac{1}{\varepsilon} - \frac{1}{\varepsilon_m}\right)$ versus $\ln(T - T_m)$ of BZT100x ceramics; (a) x = 0.025, (b) x = 0.050, (c) x = 0.075, (d) x = 0.100, (e) x = 0.125 and (f) x = 0.150.....	81
58 P-E hysteresis loop of BZT100x ceramics (a) 0.025 ≤ x ≤ 0.075 and (b) 0.100 ≤ x ≤ 0.150.....	83

LIST OF FIGURES (CONT.)

Figures	Page
59 XRD patterns of BNKLT1610 powders calcined at different temperatures: (ω) $(\text{K,Na,Li})_2\text{Ti}_6\text{O}_{13}$	89
60 SEM photographs of BNKLT1610 powders calcined at; (a) 600 °C, (b) 650 °C, (c) 700 °C, (d) 750 °C, (e) 800 °C, (f) 850 °C and (g) 900 °C.....	90
61 TEM micrographs of BNKLT1610 powders; (a) calcined at 650 °C, (b) calcined at 750 °C and (c) calcined at 850 °C.....	91
62 XRD patterns of BNKLT1610 ceramics sintered at various temperatures: (ω) $(\text{K,Na,Li})_2\text{Ti}_6\text{O}_{13}$	93
63 SEM photographs of surface BNKLT1610 ceramics sintered at; (a) 950 °C, (b) 1,000 °C, (c) 1,050 °C, (d) 1,100 °C and (e) 1,150 °C	95
64 SEM photographs of fracture BNKLT1610 ceramics sintered at; (a) 950 °C, (b) 1,000 °C, (c) 1,050 °C, (d) 1,100 °C and (e) 1,150 °C	96
65 Temperature dependences of dielectric constant and dielectric loss of the BNKLT1610 ceramics sintered at; (a) 950 °C, (b) 1,000 °C, (c) 1,050 °C, (d) 1,100 °C and (e) 1,150 °C.....	100
66 ϵ_d , ϵ_m and ϵ_r as function of sintering temperature of BNKLT1610 ceramics.....	101
67 XRD patterns of BNKLT-100xBZT ceramics with $0 \leq x \leq 0.15$	106
68 SEM photographs of surface of BNKLT-100xBZT ceramics; (a) $x = 0.025$, (b) $x = 0.050$, (c) $x = 0.075$, (d) $x = 0.100$, (e) $x = 0.125$ and (f) $x = 0.15$	107
69 Temperature dependence of dielectric constant and dielectric loss of the BNKLT-xBZT ceramics with $0.025 \leq x \leq 0.15$	109
70 ϵ_r and ϵ_{\max} as function of BZT fraction for BNKLT-xBZT ceramics with $0 \leq x \leq 0.15$	111